

1. Quality Control of Radiolabeled Folate Conjugates

1.1. Experimental Procedure

Quality control of the radiolabeled folate conjugate (**cm09**) was carried out by means of HPLC. The mobile phase consisted of an aqueous 0.05 M triethylammonium phosphate buffer pH 2.25 (A) and methanol (B) with a linear gradient from 5% B to 80% B over 25 min at a flow rate of 1mL/min.

1.2. Results

The retention time of the desired products $^{xx}\text{Tb-cm09}$ was ~ 19.7 min. Excellent radiochemical yields (> 97%) were obtained with all Tb radioisotopes (Supplemental Fig. 1-5). Traces of unreacted Tb(III) coordinated by added DTPA appeared with a retention time of 3.2 - 3.6 min. Small amounts of a radioactive side product of unknown composition were detected at a retention time of 11.4-11.7 min.

Sample information

Name	cmE182_2	Sample type	Sample
Vial #	1		
Amount	0.000000 mg	Injected volume	100.00 µl
Dilution	1	Division factor	1

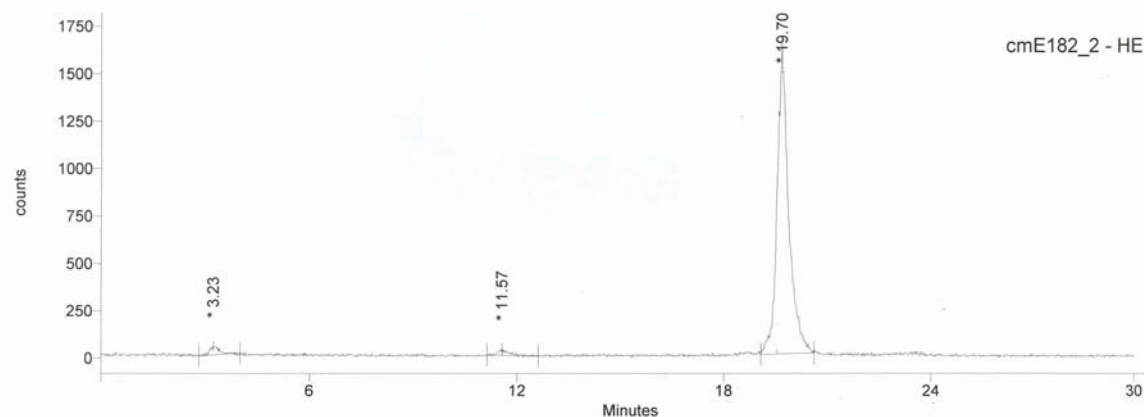
(* = original value has been modified)

Information :

Pr.7; Column 2 (XTerrea)
TEAP Buffer pH 2.25, MeOH
152Tb-DOTA-AB-folate

Integration results

#	Peak name	Rt.	Area	% Area
1		3.23	797.00	2.03
2		11.57	715.00	1.82
3		19.70	37784.50	96.15
SUM			39296.50	100.00



SUPPLEMENTAL FIGURE 1. Quality control of $^{152}\text{Tb-cm09}$ via HPLC revealed a radiochemical yield of > 96%.

Sample information

Name cmE182_4 Sample type Sample
Vial # 1
Amount 0.000000 mg Injected volume 100.00 µl
Dilution 1 Division factor 1

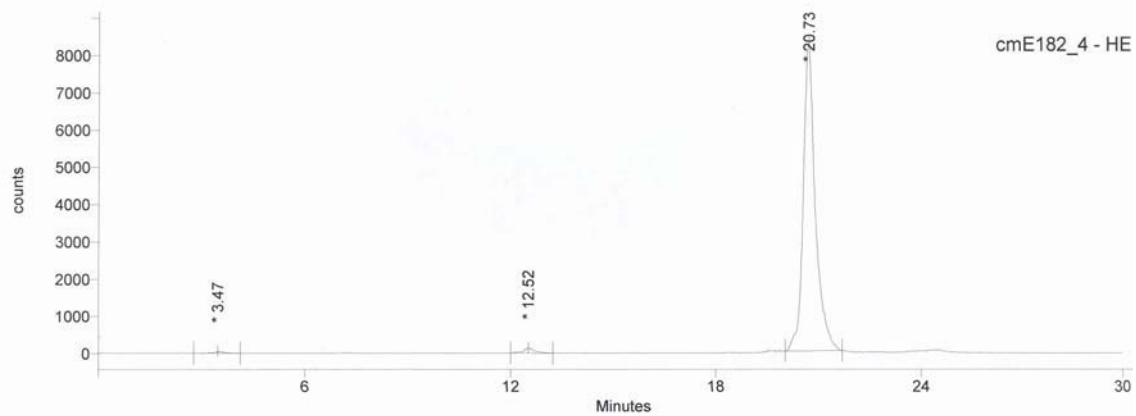
(* = original value has been modified)

Information :

Pr.7; Column 2 (XTerra)
TEAP Buffer pH 2.25, MeOH
155Tb-DOTA-AB-folate

Integration results

#	Peak name	Rt.	Area	% Area
1		3.47	1130.00	0.54
2		12.52	3121.00	1.50
3		20.73	203209.00	97.95
SUM			207460.00	100.00



SUPPLEMENTAL FIGURE 2. Quality control of $^{155}\text{Tb-cm09}$ via HPLC revealed a radiochemical yield of > 96%.

Sample information

Name	cmT018_1	Sample type	Sample
Vial #	1		
Amount	0.000000 mg	Injected volume	100.00 µl
Dilution	1	Division factor	1

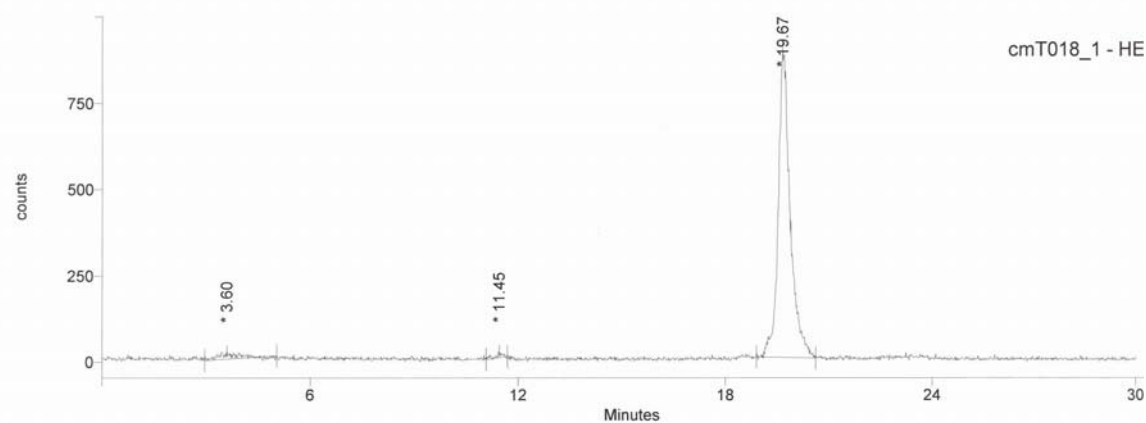
(* = original value has been modified)

Information :

Pr.7: Column 2 (XTerrea)
TEAP Buffer pH 2.25, MeOH
149Tb-DOTA-AB-folate

Integration results

#	Peak name	Rt.	Area	% Area
1		3.60	618.00	2.79
2		11.45	181.00	0.82
3		19.67	21351.00	96.39
SUM			22150.00	100.00



SUPPLEMENTAL FIGURE 3. Quality control of $^{149}\text{Tb-cm09}$ (first cycle) via HPLC revealed a radiochemical yield of > 96%.

Sample information

Name	cmT018_3	Sample type	Sample
Vial #	1		
Amount	0.000000 mg	Injected volume	100.00 µl
Dilution	1	Division factor	1

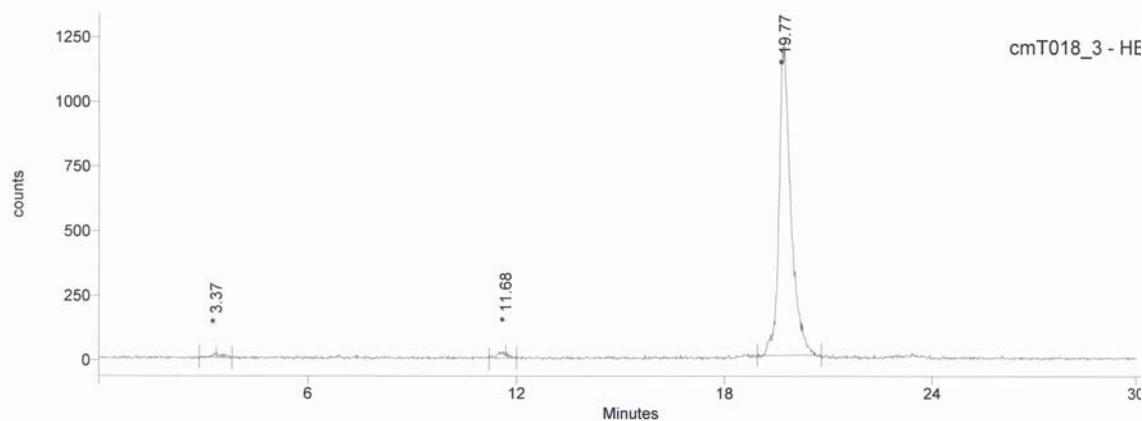
(* = original value has been modified)

Information :

Pr.7; Column 2 (XTerra)
TEAP Buffer pH 2.25, MeOH
149Tb-DOTA-AB-folate

Integration results

#	Peak name	Rt.	Area	% Area
1		3.37	283.50	0.96
2		11.68	517.00	1.75
3		19.77	28765.00	97.29
SUM			29565.50	100.00



SUPPLEMENTAL FIGURE 4. Quality control of $^{149}\text{Tb-cm09}$ (second cycle) via HPLC revealed a radiochemical yield of > 97%.

Sample information

Name	cmT024_1	Sample type	Sample
Vial #	1		
Amount	0.000000 mg	Injected volume	100.00 µl
Dilution	1	Division factor	1

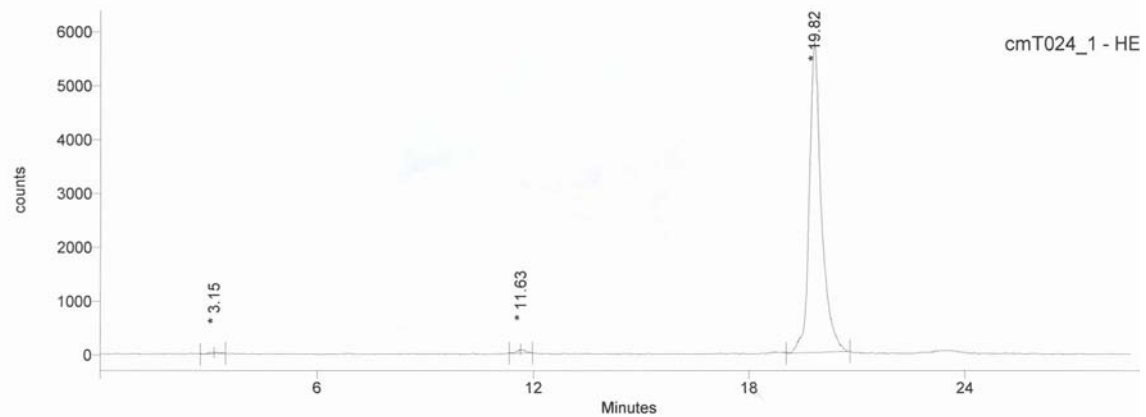
(* = original value has been modified)

Information :

Pr.7; Column 2 (XTerra)
TEAP Buffer pH 2.25, MeOH
161Tb-DOTA-AB-folate

Integration results

#	Peak name	Rt.	Area	% Area
1		3.15	548.50	0.40
2		11.63	1101.00	0.81
3		19.82	134720.00	98.79
SUM			136369.50	100.00



SUPPLEMENTAL FIGURE 5. Quality control of $^{161}\text{Tb-cm09}$ via HPLC revealed a radiochemical yield of > 98%.

2. Dosimetric Considerations of the Biological Effectiveness of ^{149}Tb and ^{161}Tb

2.1. Experimental Procedure

In order to assess the different biological effectiveness of ^{149}Tb and ^{161}Tb the relative equivalent absorbed radiation dose in tumor xenografts has been estimated for both radioisotopes. The following assumptions have been made: (i) the different physical half-lives of the radioisotopes were considered by calculation of the ratio among the integrated AUCs obtained from the biodistribution data expressed in non decay-corrected percent injected dose per gram tissue [%ID/g]. (ii) The adsorbed radiation dose of ^{149}Tb and ^{161}Tb in a sphere of 100 mg was assessed by using Unit Density Sphere Model from RADAR (www.doseinfo-radar.com). Finally, (iii) the higher relative biological effectiveness of α -particles (20) versus β^- -particles (1) was considered.

2.2. Results and Conclusion

Due to a significant difference in half-lives the ratio $^{149}\text{Tb}/^{161}\text{Tb}$ among the integrated AUCs was found to be ~ 0.066 . The self doses (Unit Density Sphere Model, RADAR) were listed as 1.16 mGy/MB \cdot s (^{149}Tb) and 0.305 mGy/MB \cdot s (^{161}Tb), respectively. Under consideration of the weighting factor for alpha-particles the $^{149}\text{Tb}/^{161}\text{Tb}$ equivalent radiation dose ratio in tumors was assumed to be ~ 68.4 .

Taken decay properties, the self dose ratio and the weighting factor for different radiation into account, we concluded that the amount of injected radioactivity should be ~ 4.5 times higher in the case of ^{161}Tb -**cm09** in order to achieve the same equivalent absorbed radiation dose in the tumor tissue as is deposited by ^{149}Tb -**cm09**.

3. SPECT and PET Images of Mice Injected with $^{155}\text{Tb-cm09}$ and $^{152}\text{Tb-cm09}$

3.1. Experimental Procedure

A KB tumor bearing nude mouse was injected with $^{155}\text{Tb-cm09}$ (3.8 MBq). Four days after injection SPECT/CT imaging was performed. Due to the limited amount of residual radioactivity the mouse was euthanized before imaging allowing the performance of a SPECT scan of 2 h duration (Suppl. Fig. 6). An in vivo PET scan of 90 min duration was performed 3 h after injection of $^{152}\text{Tb-cm09}$ (10 MBq) and compared with the PET scan of a mouse performed 24 h p.i. of $^{152}\text{Tb-cm09}$.

3.2. Results and Conclusion

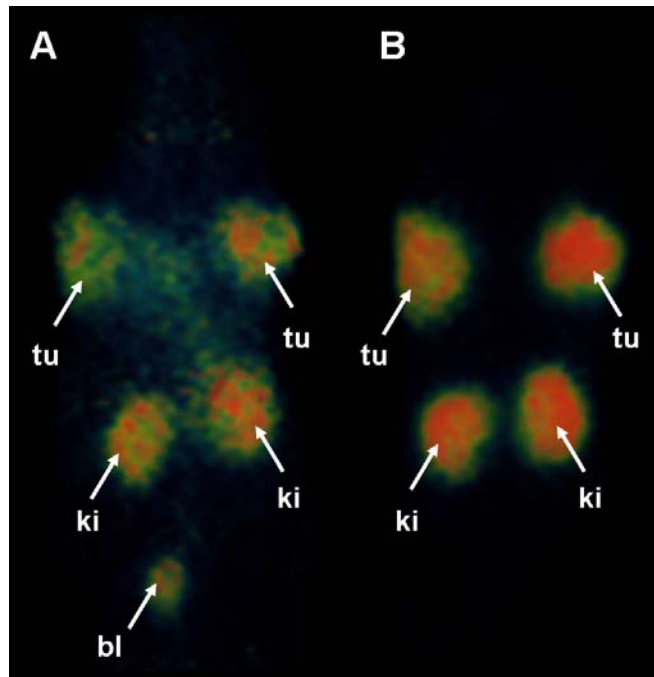
Due to the relatively long half-life (5.32 d) of ^{155}Tb this novel radioisotope would potentially allow longitudinal investigations of a radiotracer's tissue distribution profile prior to the application of radionuclide therapy through ^{149}Tb and ^{161}Tb . Even 4 days after injection of $^{155}\text{Tb-cm09}$ visualization of accumulated radioactivity in tumor xenografts and kidneys was still possible at high imaging quality via SPECT (Supplemental Fig. 6).



SUPPLEMENTAL FIGURE 6. SPECT/CT of a mouse 4 days after injection $^{155}\text{Tb-cm09}$ enabled visualization of tumor xenografts (tu) and kidney (ki).

In vivo PET imaging was also performed with a mouse 3 h after injection of $^{152}\text{Tb-cm09}$ and compared with the image obtained 24 h after injection (Suppl. Fig. 7). In agreement with the radiotracer's distribution profile determined in biodistribution studies using $^{161}\text{Tb-cm09}$ tumor-to-background contrast was increasing over time. However, already 3 h after injection tumors and

kidneys were easily distinguished from background radioactivity enabling the use of this folate PET radiotracer also for imaging purposes at early time points after injection.



SUPPLEMENTAL FIGURE 7. PET images of mice 3 h (A) and 24 h (B) after injection $^{152}\text{Tb-cm09}$ enabled visualization of tumor xenografts (tu) and kidney (ki). A small amount of radioactivity was also found in the urinary bladder (bl).

4. Availability of Enriched Gadolinium Isotopes

The suitable production routes for ^{149}Tb and ^{152}Tb are $^{152}\text{Gd}(p,4n)^{149}\text{Tb}^*$ and $^{152}\text{Gd}(p,n)^{152}\text{Tb}$ nuclear reactions, respectively. The drawback of this strategy is the low enrichment grade (~30%) of commercially available ^{152}Gd (Supplemental Table 1). The relatively high amount of stable gadolinium isotopes of mass numbers between 154 and 160 in the target material would result in accumulation of terbium radionuclide impurities, which can not be separated chemically. Therefore a higher enrichment grade of ^{152}Gd targets is needed to achieve higher quality of ^{149}Tb

* Irradiation of even highly enriched ^{152}Gd -targets would presumably result in only moderate yield and quality of ^{149}Tb due to concomitant production of side products (^{150}Tb , ^{151}Tb) and $^{149\text{m}}\text{Tb}$ which decays to ^{149}Gd .

and ^{152}Tb , produced by proton irradiations. In contrast, highly enriched ^{155}Gd (Supplemental Table 1) is commercially available and can be efficiently utilized as target material for the production of ^{155}Tb via the $^{155}\text{Gd}(p,n)^{155}\text{Tb}$ nuclear reaction.

SUPPLEMENTAL TABLE 1

Isotopic Distribution of Commercially Available Enriched Gd Isotopes

	^{152}Gd	^{154}Gd	^{155}Gd	^{156}Gd	^{157}Gd	^{158}Gd	^{160}Gd
152	30.6%	9.3%	18.1%	14.8%	8.6%	11%	7.6%
155	-	0.01%	99.82%	0.1%	0.07%	0.01%	0.005%